Disentangling acute motor deficits and adaptive responses evoked by the loss of cerebellar output

Nirvik Sinha[a,b,c], Sharon Israely[a], Ora Ben Harosh[a], Ran Harel[d], Julius PA Dewald[b,c,e,f], Yifat Prut[a]

[a]Edmond and Lily Safra Center for Brain Sciences, The Hebrew University of Jerusalem, 9190401 Jerusalem, Israel; [b]Department of Physical Therapy and Human Movement Sciences, Northwestern University Feinberg School of Medicine, Chicago, IL 60610; [c]Interdepartmental Neuroscience Center, Northwestern University Feinberg School of Medicine, Chicago, IL 60611; [d] Department of Neurosurgery, Sheba Medical Center, 5262000 Tel Aviv, Israel; [e]Department of Biomedical Engineering, Northwestern University, Evanston, IL 60208; [f] Department of Physical Medicine & Rehabilitation, Northwestern University Feinberg School of Medicine, Chicago, IL 60610

*Nirvik Sinha; *Yifat Prut

Email: Nirvik.Sinha@mail.huji.ac.il

yifat.prut@mail.huji.ac.il

Author Contributions: Y.P. designed research; N.S., S.I., O.B.H., and R.H. performed research; N.S. and S.I. analyzed the data; N.S., J.P.A.D., and Y.P. wrote the paper.

Competing Interest Statement: The authors declare no competing interest.

Classification: Major: Biological Sciences, Minor: Neuroscience

Keywords: cerebellum | nonhuman primates | coupling torques | muscle torques | motor noise

This PDF file includes:

Main Text

Figures 1 to 5

Abstract

Individuals with cerebellar deficits exhibit a broad range of motor impairments when performing voluntary movements. However, the sequence of events leading to these impairments and the distinction between primary and compensatory processes remain unclear. We addressed this question by reversibly blocking cerebellar outflow in monkeys performing planar center-out movements. We found that a reduced hand velocity observed when blocking cerebellar outflow during reaching movements is due to a decrease in muscle torque and a spatially tuned reduction in velocity, particularly pronounced during movements involving inter-joint interactions. The time course of these two processes was examined using the sequence of trials of movements to the same target when blocking cerebellar outflow. We found that during multi-joint reaching movements, the reduced velocity was driven by an acute deficit superimposed on a gradually emergent strategic slowing aimed to minimize passive inter-joint interactions. Finally, the reduction in velocity could not explain the increased motor noise observed during a cerebellar block, which manifested as decomposed and variable trajectories. Our results suggest that loss of cerebellar signals leads to motor impairments through insufficient muscle torques and altered motor control strategy to compensate for the impaired control of limb dynamics. However, impaired feedforward control also increases motor noise, which cannot be strategically eliminated.

Significance Statement

Our study examined the impact of cerebellar dysfunction on movement control by reversibly blocking the cerebellar output in monkeys. During a cerebellar block, reaching movements initially slowed due to an acute deficit in generating muscle torque. Beyond this primary deficit, there appeared to be a secondary, strategic slowing down of movements aimed at mitigating inter-joint interactions associated with rapid, ballistic movements. Finally, during the cerebellar block we observed movement variability increased independently of the reduced velocity, likely reflecting errors in movement planning. These findings highlight the role of the cerebellar in movement control and delineate the processes following cerebellar dysfunction that culminate in a broad range of motor impairments.

Main Text

Introduction

The ability to coordinate well-timed movements greatly relies on the cerebellum as evident from studies of individuals with cerebellar ataxia (1). The cerebellum regulates the timing of movements by predicting the mechanical interactions between adjacent joints (2, 3), a computation that requires an internal model of feedforward control (4-10). However, motor deficits exhibited by individuals with cerebellar deficits extend much beyond poor motor timing. For example, during the acute phase of cerebellar injury, there is a loss of muscle tone and weakness of voluntary movements (11-13). Cerebellar patients also exhibit movement-related sensory deficits such as an impaired visual perception of stimulus movement and perception of the limb position sense (i.e., proprioception or state estimation) during active movements (14, 15). Accumulating clinical data collected from cerebellar patients provide conflicting findings regarding the underlying pathophysiology resulting from a loss of cerebellar signals (16-19), most likely due to the heterogeneity of individuals with chronic cerebellar deficits, where the primary and secondary effects are inseparable. Therefore, the sequence of events leading to the observed motor impairments in cerebellar patients remains unclear.

To address this question, we trained monkeys to perform a planar reaching task with the arm supported by an exoskeleton. Cerebellar output to the motor cortex was reversibly blocked using high-frequency stimulation (HFS) through the superior cerebellar peduncle and the effect of this manipulation was measured during subsequent movements. Previously we have shown that HFS

can effectively and reversibly interfere with the normal outflow of cerebellar signals (20) since this perturbation accurately replicated the behavioral deficits identified in cerebellar patients (21) and the changes in motor cortical activity that appear after dentate cooling in monkeys (22). In the present study, we found that the loss of cerebellar outflow led to reduced hand velocity during reaching movements reflecting two parallel underlying mechanisms. First, there was a reduction in muscle torques, even for movement directions where inter-joint interactions were low. Second, the reduction in hand velocity exhibited a spatial tuning and was greater in directions that generated large inter-joint interactions, thereby reflecting an inability to compensate for limb dynamics. The time course of these two mechanisms was identified by analyzing the sequence of reaching movements to the same target during the cerebellar block. Hand velocity was low initially, reflecting a primary muscle torque deficit, and declined further in successive trials, revealing an adaptive motor strategy to minimize inter-joint interactions. Finally, we found that the decrease in velocity during cerebellar block could not fully explain the noisy and decomposed movements observed under these conditions, which may be due to an impaired state estimate of the limb that leads to the faulty feedforward control of inter-joint interactions. Taken together, we show that cerebellar output is essential for generating sufficient muscle torques to allow for fast and stereotypical movements while overcoming the complex inter-joint interactions inherent in such actions. The loss of this output triggers a sequence of early primary effects followed by compensatory responses aimed at mitigating these impairments. Together these processes result in significantly slower movements.

Results

Slower reaching movements in cerebellar block are due to weakness and impaired limb dynamics.

We trained 4 adult monkeys (*Macaca fascicularis*) to sit in a primate chair with their upper limb supported by an exoskeleton (KINARM system) and perform planar center-out movements (**Figure 1a**). The spatial location of the targets enabled us to dissociate between shoulder-dominant (lateral targets) vs. shoulder-elbow movements (diagonal and straight targets respectively).

Cerebellar block significantly reduced the ability of the monkeys to perform the task as measured by the success rate across all the recorded sessions (mean success rate in control = 86.5%, CI [85.8, 87.2] vs. cerebellar block = 75.3%, CI [73.9, 76.7], $p < 0.001$; **Supplementary table S1**). Since the monkeys had to meet strict timing criteria to perform the movements successfully during the task, we began by examining the hand kinematics**. Figure 1b** shows profiles of hand velocity in sample trials collected during the control (blue) and cerebellar block (vermillion) conditions. This example shows that movements exhibited a significant reduction in the peak hand velocity during cerebellar block. However, when compared across the targets, we found that the reduction in hand velocity was strongly modulated by the target direction (1-way ANOVA of the change in peak hand velocity, the effect of cerebellar block: $p = 0.01$, the effect of targets: $p < 0.001$; **Supplementary table S2**). *Post hoc* comparisons further revealed that the effect of cerebellar block on reaching movements i.e., movements to targets 1-4 was significantly higher than on retrieval movements i.e., movements to targets 5-8 (**Figure 1c**; mean decrease of 9.7%, CI [8.2, 11.2], $p < 0.001$ for targets 1-4 compared to mean decrease of 2.5%, CI [0.9, 4.0], $p = 0.21$ for targets 5-8) even though there was no difference in the peak hand velocity between the movements to the two target groups during control ($p = 0.88$, **Supplementary tables S3a and b**).

In the task used in our study, hand movements were made by controlling the muscle torque at the shoulder and elbow joints (23). However, simultaneous movements of both joints also generated coupling torques due to passive interactions between limb inertial properties and joint velocities (24, 25). To identify the target-specific muscle and coupling torques, we employed an inverse dynamics model of the upper limb (26) which enabled us to distinguish between the

different contributions to the net torque experienced by each joint. According to this model, the net torque at each joint is the sum of both the active muscle torque and the passive coupling torque acting at that joint (see Methods section for details).

Using the inverse dynamics model, we found that the target-specific reduction in hand velocities was produced by changes in muscle commands (e.g., **Figures 2a, b**). Specifically, we observed that the muscle torque impulses, calculated by integrating the torque profiles over the early phase of movements when acceleration was positive, were reduced in a target-specific manner during the cerebellar block (**Figure 2c**; **Supplementary table S4-5**). This reduction was particularly pronounced at the shoulder joint. Furthermore, as in the case of hand velocities, *post hoc* comparisons revealed that the shoulder joint experienced a significantly greater reduction in muscle torque for targets 1-4 vs. 5-8 (**Figure 2d**; mean decrease of 10.6%, CI [9.0, 11.2], $p < 0.001$ for targets 1-4 compared to mean decrease of 3.3%, CI [-1.3, 5.2] $p = 0.21$ for targets 5-8). In contrast, the slight reduction in elbow torques due to the cerebellar block did not reach significance for any of the targets (**Figure 2e**). Collectively, these findings indicate that during the cerebellar block, there is a reduction in shoulder muscle torque specifically for targets involved in reaching movements, which leads to the target-specific reduction in hand velocity.

Several studies have shown that individuals with cerebellar deficits exhibit an inability to correctly compensate for inter-joint interactions (16, 17). Therefore, we asked whether the reduction in muscle torques and hand velocities due to the cerebellar block could be associated with the coupling torques generated during movements in various directions. **Figures 3a and b** shows the coupling torque profiles at the shoulder and elbow joints respectively during sample trials. We observed that the coupling torque impulses varied in a target-dependent manner during both the control and cerebellar block conditions (**Figure 3c**). Furthermore, the reduction in peak hand velocities during cerebellar block was correlated to the net coupling torque impulse (calculated as the sum of absolute coupling torque impulses at both joints) during control, particularly for the reaching movements (**Figure 3d;** targets 1-4: $\rho = 0.33$, CI [0.25, 0.38], $p < 0.001$). This indicated that the effect of the cerebellar block on hand velocity during reaching movements was strongest for targets with high coupling torques. Nevertheless, despite the significant correlation between the reduced hand velocity and coupling torques, cerebellar block reduced the hand velocity even in the single-joint reaching movements (i.e., movements to target 1, mean reduction in hand velocity = 5.8%, CI [2.8, 8.7], $p < 0.001$) where the elbow was stationary. This finding indicated a reduction in the motor command which occurred in addition and beyond the effect attributable to coupling torques alone.

Overall, cerebellar block significantly impacted the kinematics and dynamics of reaching movements but not retrieval movements. Specifically, the cerebellar block caused slower hand velocities due to a systematic, target- and joint-specific reduction in muscle torques for reaching movements, which strongly correlated with the coupling torques. Additionally, a reduction in muscle torques was also observed during the single-joint reaching movements, indicating an additional component of muscle torque insufficiency that further exacerbated motor impairment following the block.

Hand velocity exhibits an adaptive trend during repeated movements to the same target during cerebellar block.

The advantage of using a reversible cerebellar block in an animal model is the ability to track the temporal profile of motor impairments induced by this condition, allowing us to distinguish between primary and compensatory effects. To this end, we assessed changes in hand kinematics produced by the cerebellar block across successive trials. Specifically, we examined the evolution of peak hand velocities for single-joint (target 1) vs. dual-joint reaching movements (data pooled for movements to targets 2-4) during blocks of control and cerebellar block trials. **Figure 4a** illustrates this procedure. Since the targets were presented in a pseudorandom order during each block of trials, we collected for each block the tested target, while keeping its order of

presentation to generate a temporally accurate sequence of trials all directed towards the same single target.

We found that during the control condition, peak hand velocity remained stable across successive trials. In contrast, cerebellar block affected hand velocity in a trial- and target-dependent manner (**Figure 4b, c**). For movements to target 1 (i.e., single-joint movements), hand velocity was lower than control but unaffected by the temporal sequence of target presentation (trial type × trial sequence interaction effect: $p = 0.69$, **Supplementary Table S6**). However, for movements to targets 2-4, hand velocity was lower than control in the early trials and declined further with successive trials (trial type × trial sequence interaction effect: $p = 0.007$, **Supplementary Table S7**).

To further quantify the effect of trial sequence on movements to targets 2-4, we performed *post hoc* comparisons (**Figure 4d**). These comparisons revealed that during the cerebellar block, hand velocity was 4.3% (CI [1.0, 7.3], $p < 0.001$) lower than control during the first 1-2 trials. With successive trials, the hand velocity declined further before reaching an asymptote during the late trials 11-20 at 8.2% (CI [5.7, 10.7], $p < 0.001$) lower than the control.

Taken together these results reveal that the hand velocity of dual-joint reaching movements during cerebellar block was already low initially, reflecting a primary deficit. Over and above this, there was a further progressive decline of the hand velocity during successive movements most likely due to an adaptive response to the inability to compensate for coupling torques. Furthermore, this adaptive response was not observed in the case of single-joint movements where the coupling torques were low, and therefore inter-joint interactions did not play a significant role.

Slow movements during the cerebellar block cannot fully account for the impaired motor timing.

Individuals with cerebellar deficits suffer from poorly timed movements, including asynchronous activation of joints during multi-joint movements leading to movement decomposition (16) or spatial variability in their movement trajectories across trials (27). However, these properties of movement are also velocity-dependent (16, 28). Therefore, it is conceivable that the combination of primary deficit and adaptive reduction in velocity to reduce the effects of coupling torque observed in our results is the main driver of abnormal motor timing. To test this, we examined movement decomposition and trajectory variability during reaching movements (which exhibited a significant reduction in hand velocity during cerebellar block) and measured the impact of hand velocity on these measures.

To quantify movement decomposition, we normalized the movement times of individual trials to range from 0 to 1 and identified the bins where either the shoulder or the elbow joint paused (angular velocity < 20°/s) while the other joint continued moving (16). In control trials, decomposition was primarily observed during the early phase of movement, where joint velocities are low making this measure more sensitive (**Figure 5a**). However, during cerebellar block trials, decomposition occurred throughout the movement (**Figure 5b**) similar to individuals with cerebellar deficits (16). To quantify this effect, we calculated a decomposition index for each trial, representing the proportion of movement time during which the movement was decomposed, as defined above. Overall, the cerebellar block increased movement decomposition by 53.5% (CI [42.2, 66.0], $p < 0.001$). Next, we asked whether movement decomposition was mainly due to lower hand velocities. We therefore selected a subset of control trials that matched the cerebellar block trials in their peak velocities. However, even though movement decomposition in these control trials was higher (11.0%, CI [5.2, 17.0], $p = 0.03$) compared to all control trials, it was still significantly lower ($p < 0.001$) than the velocity-matched cerebellar block trials (in three out of the four monkeys as shown in **Figure 5c**). This indicates that even at matched velocities, movements during cerebellar block were more decomposed relative to the control.

Next, we assessed the effect of cerebellar block and hand velocity on trajectory variability. To this end, we first aligned the hand trajectories to have the same starting position, and then rotated them so that their endpoint was located on the positive Y-axis (**Figure 5d**). Subsequently, we defined the error in each trajectory as the maximal perpendicular distance from the Y-axis. The standard deviation of the errors across all trials was used to quantify the trial-to-trial trajectory variability. Normally, slower movements are also less variable due to the speed-accuracy tradeoff (29). Therefore, we selected the subset of control trials that matched the cerebellar block trials in their peak velocities. Indeed, the trajectory variability in this subset of slower control trials was 5.5% (CI [0.9, 9.9], $p = 0.02$) lower than that of all control trials. However, when we compared the subset of velocity matched control and cerebellar block trials, we found that cerebellar block exhibited 34.6% (CI [26.2, 43.2], $p < 0.001$) higher trajectory variability (**Figure 5e)**. In other words, despite slower movements, cerebellar block increased trajectory variability.

Discussion

Individuals with cerebellar deficits exhibit altered motor behavior related mostly to poor timing and coordination of voluntary movements. Understanding the impairments that follow cerebellar lesions is often complicated by the fact that the studies of this question mostly rely on a heterogeneous population due to different levels and types of cerebellar pathologies. Here we addressed this question by using high-frequency stimulation to reversibly block cerebellar output to the motor cortex in behaving monkeys wearing an exoskeleton (20) and comparing the post-block motor behavior to control conditions. Our results indicate that cerebellar block leads to decreased hand velocity during reaching movements via two mechanisms: a reduction in muscle torques suggesting motor weakness, and spatially tuned decreases in velocity in targets where large inter-joint interactions occur, indicating a failure to compensate for limb dynamics. Analyzing the time course of these impairments revealed partially overlapping processes: an initial reduction in hand velocity due to the inability to generate sufficient muscle torques, followed by a further progressive decline in hand velocities during subsequent movements during the cerebellar block. This secondary decline was observed only in the case of dual-joint movements, suggesting an adaptive strategy to minimize inter-joint interactions. Finally, we observed increased motor noise in terms of movement decomposition and trial-to-trial trajectory variability which were independent of the slower movements observed during the cerebellar block.

Target-dependent reduction in hand velocity and coupling torques during reaching movements during the cerebellar block.

Cerebellar block led to a target-specific reduction in hand velocity, even though the arm was fully supported by the exoskeleton and thus limb support did not play any role. This observation replicates findings made in previous studies that have documented the slowing of movements in individuals with cerebellar lesions (30-32) as well as in monkeys that underwent dentate cooling (33). It was argued that the reduction in hand velocity may be a compensatory strategy to counteract the impaired ability to manage inter-joint coupling torques in the absence of cerebellar input to the motor cortex (16, 30, 34, 35). Since coupling torques in multi-joint movements are generated in a velocity-dependent manner (24, 36), slowing down the movement not only simplifies its kinetics (by reducing the impact of coupling torques) but also allows more time for slower visual feedback to aid in guiding the movement (37). Our findings, which demonstrate a correlation between the extent of hand velocity reduction during cerebellar block and the magnitude of coupling torque under control conditions, further corroborate this hypothesis and confirms our approach for reversible inactivation of cerebellar output as a model for ataxia. Furthermore, our model enabled us to study this effect rigorously and systematically while dissociating it from the other primary effects of cerebellar block as discussed below.

Muscle torque deficit is an acute response to the cerebellar block.

Poor compensation for coupling torque is a fundamental deficit in cerebellar ataxia (17). However, early studies have reported the occurrence of muscle weakness (asthenia) and hypotonia acutely following cerebellar injury in humans (38) or experimental lesions in animals (39-42). Both Luciani (39) and Holmes (13) described a triad of cerebellar deficits to be atonia (low muscle tone), asthenia (weakness of voluntary movements), and astasia (oscillation of the head and trunk). Importantly, muscle weakness is typically characteristic of the acute phase of injury, especially in the upper extremity, and tends to normalize gradually over weeks to months, depending on the severity of the injury (43). It is therefore conceivable that studies in humans with cerebellar deficits, which often included subjects at the chronic stage of the lesion, may have underestimated the contribution of muscle weakness which by that time was already less pronounced.

We explored the acute outcome of the cerebellar block, a phase in which muscle weakness may play a more prominent role. Importantly, we showed that muscle torque deficits appear immediately after the cerebellar block, resulting in lower hand velocity already in the first few trials of both single- and dual-joint movements. This kind of fast response is less likely to be a strategic response aimed at mitigating the loss of cerebellar signals. This finding is consistent with the initial weakness followed by a gradual recovery of function observed in acute lesions of other neural structures involved in movement control, including the primary (44) and premotor cortices (45, 46). It also aligns with the understanding that cerebellar output provides a strong excitatory drive to the motor cortex (47-49) and several subcortical descending motor systems (50), beyond its well-known role in motor timing and coordination. Following the initial reduction in hand velocity observed in our study, there was a further gradual decline across subsequent trials specifically for the dual-joint movements, a behavior profile that is more consistent with strategic effort, most likely in response to the inability to compensate for limb dynamics.

Therefore, the slower movements in the absence of cerebellar signals are likely due to two main factors: (i) a primary inability to generate sufficient muscle torques due to the lack of synchronized recruitment of the cortical and sub-cortical descending motor systems via the cerebellar output, and (ii) a secondary adaptive strategy aimed at compensating for the impaired prediction of limb dynamics due to the loss of feedforward control signals from the cerebellum.

Insufficient muscle torques vs. poor inter-joint coordination

Unlike most previous clinical studies that examined motor deficits in individuals with chronic cerebellar injuries, our study utilized a reversible model of cerebellar block. This approach enabled us to track the temporal evolution of motor deficits from the onset of the block within the same study participant. Although several studies have explored the nature of motor deficits following cerebellar injuries, there remains considerable debate regarding the fundamental mechanisms driving these deficits. Some studies have suggested that the inability to compensate for inter-joint interactions is the primary driver of the observed motor abnormalities in cerebellar injury (16, 17). In contrast, other studies have emphasized the inability to generate sufficient muscle torques as the core deficit in cerebellar ataxia while claiming that inter-joint coordination is unaffected following cerebellar lesions (18, 19). Given these conflicting findings, our study aimed to systematically explore the entire spectrum of motor deficits using a model of reversible cerebellar block. First, we found that the deficits in muscle torque are more pronounced for the reaching movements as compared to the retrieval movements. We identified both an acute insufficiency in muscle torque generation and the inability to compensate for coupling torques as potential mechanisms underlying the observed slowness during the reaching movements. Moreover, we delineated the time course of these deficits, providing insights into their evolution from the onset of cerebellar block.

The asymmetric effect of cerebellar block on reaching vs. retrieval movements

We observed a notable distinction in the impact of cerebellar blockage on reaching vs. retrieval movements. At a collective level, this variance could be attributed to the disparity in magnitude of coupling torque impulse, with movements towards targets 2-4 exhibiting 18.7% (CI [13.1, 24.1], p = 0.008) higher coupling torque impulse compared to those towards targets 6-8. However, this explanation does not consistently hold when examined at the individual target level. For instance, while the coupling torque was higher for movements towards target 7, the effects of cerebellar blockage were less pronounced compared to those observed for target 1, where the coupling torques are considerably lower. There are two possible explanations for this discrepancy. One possibility is that the effect of cerebellar block exhibits a bias in the direction of shoulder flexion (i.e., for movements to targets 1-4). In fact, early studies in cats (51, 52), non-human primates (53) and humans (54) have reported activation of ipsilateral flexors of the arm following stimulation of the deep cerebellar nuclei and the superior cerebellar peduncle. Furthermore, lesioning of these structures led to the reduction of ipsilateral flexor tone and power (54, 55). The cerebellar output influences the excitability of spinal interneurons either directly (56-58) or via indirect relays in the subcortical descending motor systems like the rubrospinal and the reticulospinal pathways (50). Since the spinal interneurons influence the activity of flexor muscles twice as often as extensor muscles (59), this might explain why the cerebellar block had a stronger effect on movements involving shoulder flexion relative to shoulder extension in our study. Alternatively, the initial position of the limb in our experimental setup (i.e., on the central target) might have been favorable for movements in the direction of shoulder extension, thereby making them easier to perform.

Asynchronous joint movements and motor variability are unaffected by the movement velocity in cerebellar block.

Abnormally high motor variability (27, 60, 61) and decomposition of multi-joint movements (16) are core deficits in cerebellar patients. We showed that the cerebellar block decomposed the dual-joint movements into temporally isolated single-joint actions and led to an increased trial-to-trial spatial noise. These two measures can be affected by the reduction in movement velocities. Our results showed that even though movement decomposition increased with a reduction in velocity in control trials, they were still significantly lower than that of velocity-matched cerebellar block trials. Second, the trial-to-trial spatial noise in hand trajectories increased during cerebellar block despite the slower movement speeds. The cerebellum is known to participate in the planning of movements by providing an internal model of the limb which is necessary for predicting the sensory outcomes of motor commands (4). For this purpose, the cerebellum aids in estimating the state of the limb by integrating the sensory information of its last known state with predictions of its response to the latest motor command (62, 63). Therefore, in the absence of cerebellar signals, there are programming errors in the feedforward command required to launch the limb accurately toward a target (27). These feedforward errors may in turn translate into the noisy joint activation patterns and variable hand trajectories observed in our results. Moreover, the persistence of these deficits independently of the movement speeds observed during cerebellar block indicates that they cannot be compensated for, unlike the impaired prediction of inter-joint interactions which are strategically dealt with by reducing the movement velocity.

In summary, our study systematically investigated the temporal progression and distinct mechanisms of motor deficits in a controlled, reversible animal model of cerebellar block. These include an acute onset muscle torque deficit, impaired compensation of limb dynamics, and increased motor noise. We aim to further explore the neural correlates of these deficits in future studies.

Materials and Methods

Experimental subjects

This study was performed on four adult female monkeys (*Macaca fascicularis*, weight 4.5-8 kg). The care and surgical procedures of the subjects will be in accordance with the Hebrew University Guidelines for the Use and Care of Laboratory Animals in Research, supervised by the Institutional Committee for Animal Care and Use.

Behavioral task

Each monkey was trained to sit in a primate chair and perform planar, center-out movements. During the task, the left upper arm was abducted 90° and rested on cushioned troughs secured to links of a two-joint exoskeleton (KINARM, BKIN Technologies Ltd.). The sequence of events in each trial of this task was as follows. First, the monkey located a cursor (projected on a horizontal screen immediately above its arm) within a central target. After 500-800 ms, a randomly selected peripheral target (out of 8 evenly distributed targets) was displayed. The monkey had to wait until the central target disappeared (i.e., the 'go' signal) and then reach the cued peripheral target. This delay between the cue and the 'go' signal was 450-600 ms. The monkey was rewarded with a drop of applesauce if it moved the cursor to the correct target within 1 s of the 'go' signal.

Insertion of the stimulating electrode into the superior cerebellar peduncle

After the training was completed, a square recording chamber (24x24 mm) was attached to the monkey's skull above the upper limb-related area of the motor cortex in a surgical procedure under general anesthesia. To insert a chronic stimulating electrode into the ipsilateral superior cerebellar peduncle (SCP), a round chamber (diameter = 19 mm) was also implanted above the estimated insertion point (as per stereotactic measurements) during the surgery for the cortical chamber implantation. Subsequently, a post-surgery MRI was used to plan the trajectory for the electrode insertion into the SCP. After a recovery and re-training period, a bi-polar concentric electrode (Microprobes for Life Science Inc.) was inserted through the round chamber along the planned trajectory. During the process of insertion, the evoked multi-unit activity in the primary motor cortex was simultaneously monitored to identify the precise location where the stimulating electrode should be secured (47, 64).

High frequency stimulation to block the cerebellar outflow to the motor cortex

The superior cerebellar peduncle was blocked using high-frequency stimulation (HFS). This stimulation protocol consisted of a train of biphasic rectangular-pulse stimuli (where each phase was 200 µs) applied at 130 Hz. Each train was delivered at a fixed intensity of 150-250 µA. In our earlier study, we demonstrated that by using this manipulation we can successfully replicate the impaired motor timing and coordination characteristic of cerebellar ataxia (20). Furthermore, we also demonstrated that at the motor cortical level, this manipulation leads to a loss of response transients at movement onset and decoupling of task-related activity, similar to findings observed in studies where the dentate nucleus was cooled (22). Deep brain stimulation (DBS) is a perturbation similar in properties to the HFS we used, which is routinely used in clinical practice for similar purposes of interfering with neural circuitries that underwent pathological changes (65) although in both applications there is no accurate measure for the extent of the block (i.e., the fraction of fibers which become ineffective in these conditions) other than the behavioral consequences. HFS probably imposes only a partial block of the CTC system, but the behavioral outcomes we found here during an adaptation task further confirm the validity of this approach.

Data collection protocol

Each monkey performed the experimental task for several days (sessions). A total of 46, 29, 36, and 54 sessions of data were collected from Monkeys S, C, M, and P, respectively. Each session was divided into three or four sub-sessions. Each sub-session included blocks of control trials (~80 trials) and trials with the superior cerebellar peduncle blocked using high-frequency stimulation (~50 trials) as described above. During the task performance, the following behavioral

data was obtained at 1000 Hz using the KINARM's motor encoders: (i) Hand position in the x-y plane of movement, (ii) Elbow and shoulder joint angular positions, velocities, and accelerations. The lengths of the upper arm and forearm of each monkey were measured as the distances from the head of the humerus to the lateral epicondyle and from the lateral epicondyle to the palm respectively. The inertial properties of the upper limb were estimated using the monkey's body weight (66).

Processing of the behavioral data

All data analysis was performed in MATLAB R2021b (MathWorks Inc.). The raw kinematic data was low-passed filtered by using a second order Butterworth filter (cutoff = 10Hz) and then epoched into trials. For this purpose, the start and end events were taken as the time of presentation of the cue (i.e., the peripheral target) and the time of entry of the control cursor into the peripheral target respectively. This cutoff meant that a major portion of the extracted segment of each trial was the acceleration phase of the movement. The movement onset was defined as the time when the radial hand velocity exceeded 5% of its peak. Subsequently, all the trials were zero-centered around the calculated movement onset. We then applied a two-link inverse dynamics model of the upper arm to the kinematic data to compute the coupling and muscle torques acting on the elbow and shoulder joints (26). The inverse dynamics equations of motion for the combined system consisting of the monkey's arm and the associated moving components of the KINARM were used to compute the joint torques:

$$T_{me} = T_{ne} - T_{ce} \quad \text{(i)}$$

$$T_{ms} = T_{ns} - T_{cs} \quad \text{(ii)}$$

where T_{ne} and T_{ns} are the net torques (proportional to the joint's acceleration), T_{ce} and T_{cs} are passive coupling torques, and T_{me} and T_{ms} are the active muscle torques acting at the elbow and shoulder joints respectively. The expanded formulas for computing each of the above terms are provided by equations 1a-2e in the methods section C (26). It must be noted that the 'muscle' torques computed here include the effects of the actively generated muscle forces as well as the viscoelastic effects that result from the musculoskeletal system and the KINARM (67).

Statistical analyses

We used linear mixed effects analysis to evaluate the effects of predictor variables of interest on the computed response variables. This allowed us to account for the variability across the monkeys which was modeled as a random effect. Each data sample for this model was obtained by calculating the median of all the trials for each unique combination of the response variable(s) per session. We computed the change in the measured outcome variable due to the cerebellar block per session using the following formula:

$$\frac{Median\ response\ during\ cerebellar\ block - median\ response\ during\ control}{Median\ response\ during\ control} \times 100$$

For post-hoc comparisons, we used the 'coefTest' function from MATLAB's 'fitlme' to perform hypothesis testing on the fixed effects. This involved specifying the contrast matrices to test specific hypotheses regarding the differences in the response variables across the levels of the predictor variables. The 'coefTest' function allowed us to obtain p-values for these comparisons. The computed p-values were then corrected using the Benjamini-Hochberg procedure to control the false discovery rate for multiple post-hoc comparisons, wherever applicable (68). A significance level of 0.05 was used for all comparisons in this study. For estimation of the group means and their confidence intervals, we pooled the per session data from all monkeys after ensuring that effects are consistent across the monkeys. For further clarity, we have also

overlayed the means of the measured variables from individual monkeys on all our plots of summary statistics.

Acknowledgments

This work was funded by the Israel Science Foundation (ISF-1801/18 and ISF 1207/23) to Y.P., the Deutsche Forschungsgemeinschaft (DFG, German Research Foundation Project-ID 431549029–SFB 1451) to Y.P., the National Institutes of Health (NIH R01NS105759) to J.P.A.D., the Council for Higher Education PhD Sandwich Fellowship, Government of Israel to N.S., and the generous support of the Baruch Foundation to Y.P. The authors would like to thank Dr. Abdulraheem Nashef, a postdoctoral fellow at the University of Colorado for collecting part of the data used in this study.

References

1. H. Beppu, M. Suda, R. Tanaka, ANALYSIS OF CEREBELLAR MOTOR DISORDERS BY VISUALLY GUIDED ELBOW TRACKING MOVEMENT. *Brain* **107**, 787-809 (1984).
2. M. Manto *et al.*, Consensus Paper: Roles of the Cerebellum in Motor Control-The Diversity of Ideas on Cerebellar Involvement in Movement. *Cerebellum (London, England)* **11**, 457-487 (2011).
3. R. B. Ivry, S. W. Keele, Timing Functions of The Cerebellum. *Journal of Cognitive Neuroscience* **1**, 136-152 (1989).
4. D. M. Wolpert, R. C. Miall, M. Kawato, Internal models in the cerebellum. *Trends Cogn. Sci. (Regul. Ed.)* **2**, 338-347 (1998).
5. M. Kawato, Internal models for motor control and trajectory planning. *Current Opinion in Neurobiology* **9**, 718-727 (1999).
6. M. Shidara, K. Kawano, H. Gomi, M. Kawato, Inverse-dynamics model eye movement control by Purkinje cells in the cerebellum. *Nature* **365**, 50-52 (1993).
7. L. Popa, A. Hewitt, T. Ebner, Purkinje Cell Simple Spike Discharge Encodes Error Signals Consistent with a Forward Internal Model. *Cerebellum (London, England)* **12** (2013).
8. R. Shadmehr, F. Mussa-Ivaldi, Adaptive representation of dynamics during learning of a motor task. *The Journal of Neuroscience* **14**, 3208-3224 (1994).
9. R. L. Sainburg, C. Ghez, D. Kalakanis, Intersegmental Dynamics Are Controlled by Sequential Anticipatory, Error Correction, and Postural Mechanisms. *J. Neurophysiol.* **81**, 1045-1056 (1999).
10. D. M. Wolpert, Z. Ghahramani, M. I. Jordan, An Internal Model for Sensorimotor Integration. *Science* **269**, 1880-1882 (1995).
11. G. Holmes, THE CEREBELLUM OF MAN1. *Brain* **62**, 1-30 (1939).
12. K. Goldstein, Das Kleinhirn. *Handbuch der normalen und pathologischen Physiologie* **10**, 222-222 (1927).
13. G. Holmes, The symptoms of acute cerebellar injuries due to gunshot injuries. *Brain: A Journal of Neurology* **40**, 461-535 (1917).
14. H. M. Weeks, A. S. Therrien, A. J. Bastian, Proprioceptive Localization Deficits in People With Cerebellar Damage. *The Cerebellum* **16**, 427-437 (2017).
15. A. S. Therrien, A. J. Bastian, Cerebellar damage impairs internal predictions for sensory and motor function. *Current Opinion in Neurobiology* **33**, 127-133 (2015).
16. A. J. Bastian, T. A. Martin, J. G. Keating, W. T. Thach, Cerebellar ataxia: abnormal control of interaction torques across multiple joints. *J. Neurophysiol.* **76**, 492-509 (1996).

17. A. J. Bastian, K. M. Zackowski, W. T. Thach, Cerebellar Ataxia: Torque Deficiency or Torque Mismatch Between Joints? *J. Neurophysiol.* **83**, 3019-3030 (2000).
18. H. Topka, J. Konczak, K. Schneider, A. Boose, J. Dichgans, Multijoint arm movements in cerebellar ataxia: Abnormal control of movement dynamics. *Exp Brain Res* **119**, 493-503 (1998).
19. A. Boose, J. Dichgans, H. Topka, Deficits in phasic muscle force generation explain insufficient compensation for interaction torque in cerebellar patients. *Neuroscience Letters* **261**, 53-56 (1999).
20. A. Nashef, O. Cohen, R. Harel, Z. Israel, Y. Prut, Reversible Block of Cerebellar Outflow Reveals Cortical Circuitry for Motor Coordination. *Cell Rep* **27**, 2608-2619.e2604 (2019).
21. A. J. Bastian, Mechanisms of Ataxia. *Physical Therapy* **77**, 672-675 (1997).
22. J. Meyer-Lohmann, B. Conrad, K. Matsunami, V. B. Brooks, Effects of dentate cooling on precentral unit activity following torque pulse injections into elbow movements. *Brain Research* **94**, 237-251 (1975).
23. S. H. Scott, Optimal feedback control and the neural basis of volitional motor control. *Nature Reviews Neuroscience* **5**, 532-545 (2004).
24. J. M. Hollerbach, T. Flash, Dynamic interactions between limb segments during planar arm movement. *Biological Cybernetics* **44**, 67-77 (1982).
25. N. A. Bernshteĭn (1967) The co-ordination and regulation of movements. (Pergamon Press Oxford, Oxford).
26. A. Fagg, G. Ojakangas, L. Miller, N. Hatsopoulos, Kinetic Trajectory Decoding Using Motor Cortical Ensembles. *IEEE transactions on neural systems and rehabilitation engineering : a publication of the IEEE Engineering in Medicine and Biology Society* **17**, 487-496 (2009).
27. B. L. Day, P. D. Thompson, A. E. Harding, C. D. Marsden, Influence of vision on upper limb reaching movements in patients with cerebellar ataxia. *Brain* **121**, 357-372 (1998).
28. R. Osu, K.-i. Morishige, J. Nakanishi, H. Miyamoto, M. Kawato, Practice reduces task relevant variance modulation and forms nominal trajectory. *Scientific Reports* **5**, 17659 (2015).
29. R. Plamondon, A. M. Alimi, Speed/accuracy trade-offs in target-directed movements. *Behavioral and Brain Sciences* **20**, 279-303 (1997).
30. B. Wild, J. Dichgans, Cerebellar ataxia in ataxic hemiparesis? A kinematic and EMG analysis. *Movement Disorders* **8**, 363-366 (1993).
31. H. Topka, J. Konczak, J. Dichgans, Coordination of multi-joint arm movements in cerebellar ataxia:Analysis of hand and angular kinematics. *Exp Brain Res* **119**, 483-492 (1998).
32. J. Konczak, B. Schoch, A. Dimitrova, E. Gizewski, D. Timmann, Functional recovery of children and adolescents after cerebellar tumour resection. *Brain* **128**, 1428-1441 (2005).
33. T. Tsujimoto, H. Gemba, K. Sasaki, Effect of cooling the dentate nucleus of the cerebellum on hand movement of the monkey. *Brain Research* **629**, 1-9 (1993).
34. A. J. Bastian, W. T. Thach, Cerebellar outflow lesions: A comparison of movement deficits resulting from lesions at the levels of the cerebellum and thalamus. *Annals of Neurology* **38**, 881-892 (1995).

553 35. R. F. Beer, J. P. A. Dewald, W. Z. Rymer, Deficits in the coordination of multijoint arm
554 movements in patients with hemiparesis: evidence for disturbed control of limb
555 dynamics. *Exp Brain Res* **131**, 305-319 (2000).
556 36. N. Virji-Babul, J. D. Cooke, Influence of joint interactional effects on the coordination of
557 planar two-joint arm movements. *Exp Brain Res* **103**, 451-459 (1995).
558 37. M. Jeannerod, *The neural and behavioural organization of goal-directed movements*,
559 The neural and behavioural organization of goal-directed movements. (Clarendon
560 Press/Oxford University Press, New York, NY, US, 1988), pp. xii, 283-xii, 283.
561 38. D. E. Haines, M.-U. Manto, M. Glickstein, Clinical symptoms of cerebellar disease and
562 their interpretation. *The Cerebellum* **6**, 141-156 (2007).
563 39. L. Luciani, Il Cervelletto. Nuovi Studi di Fisiologia Normale e Patologica. *Philosophical*
564 *Review* **2** (1893).
565 40. F. Bremer, G.-H. Roger, L. Binet, Le cervelet. *Traité de physiologie*, 39-134 (1935).
566 41. J. F. Fulton, R. S. Dow, The Cerebellum: A Summary of Functional Localization *. *The Yale*
567 *Journal of Biology and Medicine* **10**, 89 - 119 (1937).
568 42. R. Granit, B. Holmgren, P. A. Merton, The two routes for excitation of muscle and their
569 subservience to the cerebellum. *The Journal of Physiology* **130**, 213-224 (1955).
570 43. J. Konczak *et al.*, Recovery of Upper Limb Function After Cerebellar Stroke. *Stroke* **41**,
571 2191-2200 (2010).
572 44. P. Pressman, H. J. Rosen, "Chapter 33 - Disorders of Frontal Lobe Function" in
573 Neurobiology of Brain Disorders, M. J. Zigmond, L. P. Rowland, J. T. Coyle, Eds.
574 (Academic Press, San Diego, 2015), https://doi.org/10.1016/B978-0-12-398270-4.00033-
575 1, pp. 542-557.
576 45. H. J. Freund, H. Hummelsheim, Lesions of premotor cortex in man. *Brain : a journal of*
577 *neurology* **108 (Pt 3)**, 697-733 (1985).
578 46. H.-J. Freund, Clinical aspects of premotor function. *Behavioural Brain Research* **18**, 187-
579 191 (1985).
580 47. A. Nashef, O. Cohen, Z. Israel, R. Harel, Y. Prut, Cerebellar Shaping of Motor Cortical
581 Firing Is Correlated with Timing of Motor Actions. *Cell Rep* **23**, 1275-1285 (2018).
582 48. Y. Shinoda, M. Yamazaki, T. Futami, Convergent inputs from the dentate and the
583 interpositus nuclei to pyramidal tract neurons in the motor cortex. *Neuroscience Letters*
584 **34**, 111-115 (1982).
585 49. J. Hore, D. Flament, Changes in motor cortex neural discharge associated with the
586 development of cerebellar limb ataxia. *J. Neurophysiol.* **60**, 1285-1302 (1988).
587 50. T. J. H. Ruigrok, "Cerebellar Influences on Descending Spinal Motor Systems" in
588 Handbook of the Cerebellum and Cerebellar Disorders, M. Manto, J. D. Schmahmann, F.
589 Rossi, D. L. Gruol, N. Koibuchi, Eds. (Springer Netherlands, Dordrecht, 2013),
590 10.1007/978-94-007-1333-8_23, pp. 497-528.
591 51. W. K. Hare, H. W. Magoun, S. W. Ranson, ELECTRICAL STIMULATION OF THE INTERIOR
592 OF THE CEREBELLUM IN THE DECEREBRATE CAT. *American Journal of Physiology-Legacy*
593 *Content* **117**, 261-266 (1936).
594 52. W. W. Chambers, Jr., Electrical stimulation of the interior of the cerebellum in the cat.
595 *Am. J. Anat.* **80**, 55-93 (1947).
596 53. H. W. Magoun, W. K. Hare, S. W. Ranson, ELECTRICAL STIMULATION OF THE INTERIOR
597 OF THE CEREBELLUM IN THE MONKEY. *American Journal of Physiology-Legacy Content*
598 **112**, 329-339 (1935).

54. B. S. Nashold, D. G. Slaughter, Effects of Stimulating or Destroying the Deep Cerebellar Regions in Man. *Journal of Neurosurgery* **31**, 172-186 (1969).
55. R. C. Schneider, E. C. Crosby, The Interplay Between Cerebral Hemispheres and Cerebellum in Relation to Tonus and Movements. *Journal of Neurosurgery* **20**, 188-198 (1963).
56. H. Bantli, J. R. Bloedel, The action of the dentate nucleus on the excitability of spinal motoneurons via pathways which do not involve the primary sensorimotor cortex. *Brain Research* **88**, 86-90 (1975).
57. A. Sathyamurthy *et al.*, Cerebellospinal Neurons Regulate Motor Performance and Motor Learning. *Cell Rep* **31**, 107595 (2020).
58. C. Asanuma, W. T. Thach, E. G. Jones, Nucleus interpositus projection to spinal interneurons in monkeys. *Brain Research* **191**, 245-248 (1980).
59. S. I. Perlmutter, M. A. Maier, E. E. Fetz, Activity of Spinal Interneurons and Their Effects on Forearm Muscles During Voluntary Wrist Movements in the Monkey. *J. Neurophysiol.* **80**, 2475-2494 (1998).
60. D. Timmann, S. Watts, J. Hore, Failure of Cerebellar Patients to Time Finger Opening Precisely Causes Ball High-Low Inaccuracy in Overarm Throws. *J. Neurophysiol.* **82**, 103-114 (1999).
61. J. E. Schlerf, J. Xu, N. M. Klemfuss, T. L. Griffiths, R. B. Ivry, Individuals with cerebellar degeneration show similar adaptation deficits with large and small visuomotor errors. *J. Neurophysiol.* **109**, 1164-1173 (2012).
62. R. C. Miall, L. O. D. Christensen, O. Cain, J. Stanley, Disruption of State Estimation in the Human Lateral Cerebellum. *PLOS Biology* **5**, e316 (2007).
63. R. C. Miall, D. King, State Estimation in the Cerebellum. *The Cerebellum* **7**, 572-576 (2008).
64. A. Nashef, H. Rapp, M. P. Nawrot, Y. Prut, Area-specific processing of cerebellar-thalamo-cortical information in primates. *Biological Cybernetics* **112**, 141-152 (2018).
65. J. S. Perlmutter, J. W. Mink, DEEP BRAIN STIMULATION. *Annu. Rev. Neurosci.* **29**, 229-257 (2006).
66. E. J. Cheng, S. H. Scott, Morphometry of Macaca mulatta forelimb. I. Shoulder and elbow muscles and segment inertial parameters. *Journal of Morphology* **245**, 206-224 (2000).
67. J. L. Smith, R. F. Zernicke, Predictions for neural control based on limb dynamics. *Trends Neurosci* **10**, 123-128 (1987).
68. W. Haynes, "Benjamini–Hochberg Method" in Encyclopedia of Systems Biology, W. Dubitzky, O. Wolkenhauer, K.-H. Cho, H. Yokota, Eds. (Springer New York, New York, NY, 2013), 10.1007/978-1-4419-9863-7_1215, pp. 78-78.

Figures and Tables

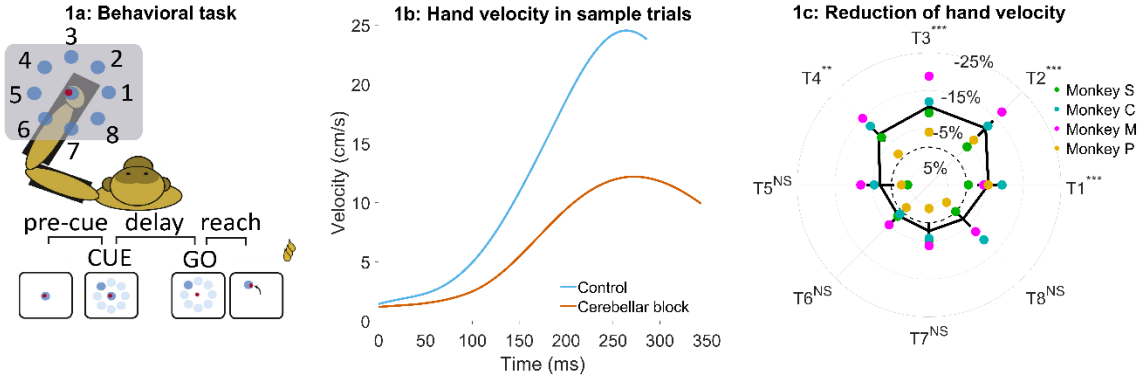

Figure 1: Effect of cerebellar block on peak hand velocity. (a) Schematic of the monkey performing the delayed reaching task in the KINARM exoskeleton to eight peripheral targets on the horizontal plane. The locations of the eight targets are numbered. (b) Movement-onset aligned hand velocity profiles during a sample control and cerebellar block trial performed by monkey C to target 2. Entry of the control cursor into the peripheral target marked the end of the trial. (c) Target-wise effect of the cerebellar block on peak hand velocity. For each session, the target-wise reduction in the median peak hand velocity during the cerebellar block trials was computed relative to that of control trials. The depicted values are the means ± 95% confidence intervals across all sessions pooled from all the four monkeys. The means of individual monkeys are overlaid. The dashed circle indicates no change. Statistical significance is denoted as follows: $p \geq 0.05^{NS}$, $p < 0.05^{*}$, $p < 0.01^{**}$, $p < 0.001^{***}$. [T1-8: Targets 1-8]

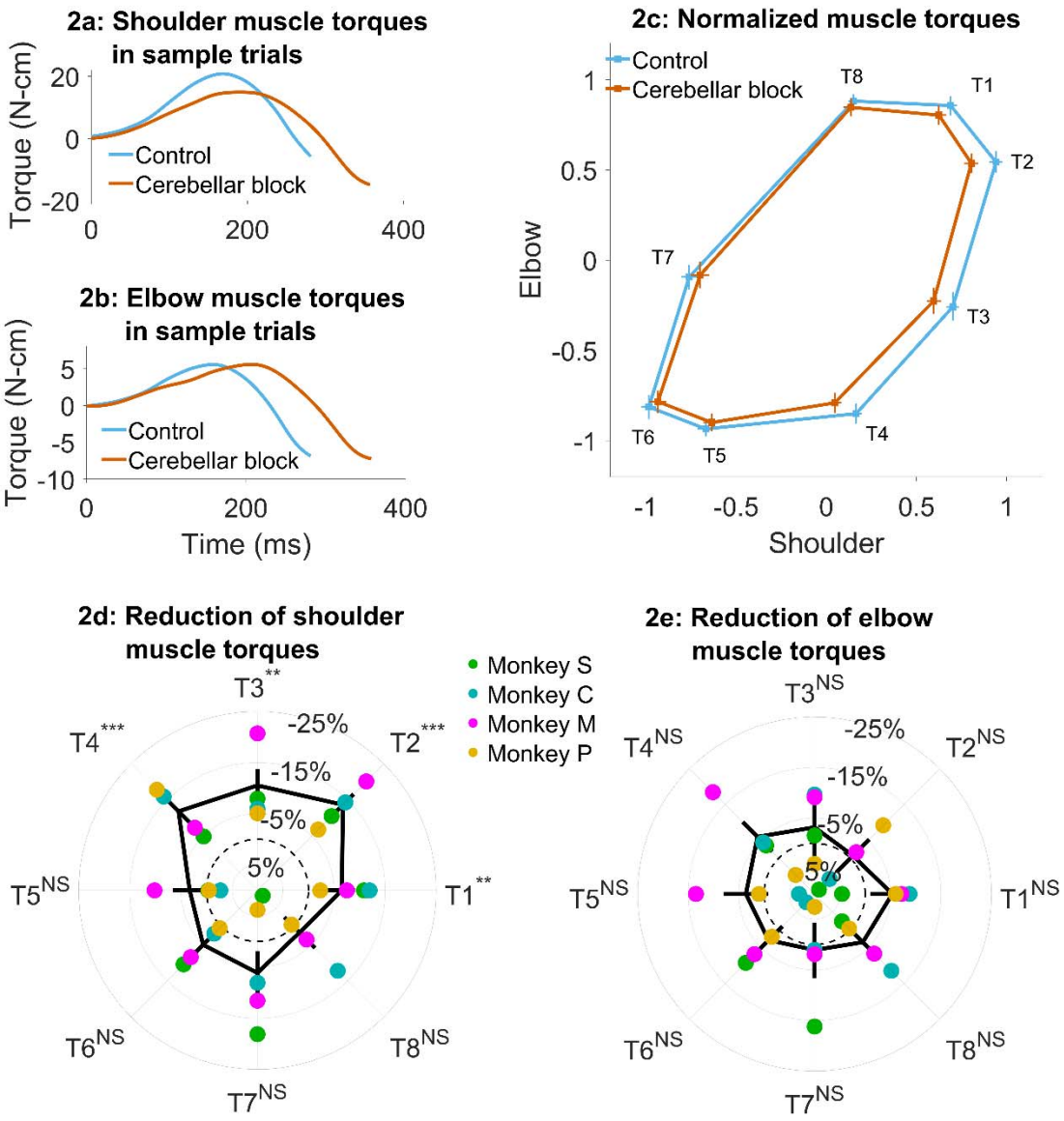

Figure 2: Effect of cerebellar block on muscle torques. Movement-onset aligned shoulder (a) and elbow (b) muscle torque profiles during a sample control and cerebellar block trial performed by monkey C to target 2. Entry of the control cursor into the peripheral target marked the end of the trial. (c) Normalized muscle torque impulse at the shoulder vs. elbow per target during control and cerebellar block. For each session, we computed the target-wise median muscle torque impulse during the acceleration phase of the movement across the control and cerebellar block trials. They were then normalized by the maximum absolute torque impulse across all the targets. The depicted values are the means across all the sessions pooled from the data of all four monkeys. The 95% confidence interval of the means is indicated by the horizontal and vertical bars for the shoulder and elbow joints respectively. Target-wise effect of cerebellar block on shoulder (d) and elbow (e) muscle torque impulse. For each session, the target-wise reduction in the median torque impulse during the cerebellar block trials was computed relative to the maximum absolute value of the target-wise medians observed during the control trials. The depicted values are the means ± 95% confidence intervals across all sessions pooled from all four monkeys. The means of individual monkeys are overlaid. The dashed circle indicates no

change. Statistical significance is denoted as follows: $p \geq 0.05^{NS}$, $p < 0.05$*, $p < 0.01$**, $p < 0.001$***. [T1-8: Targets 1-8]

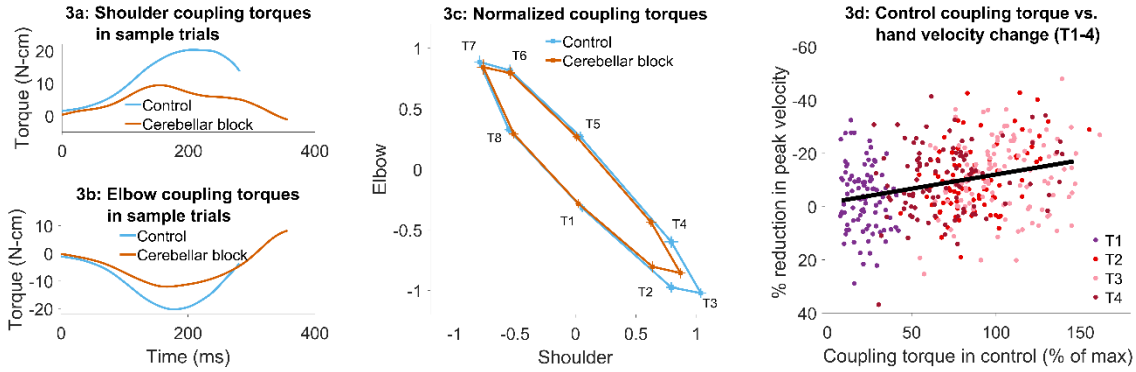

Figure 3: Effect of cerebellar block on coupling torques. Movement-onset aligned shoulder (a) and elbow (b) coupling torque profiles during a sample control and cerebellar block trial performed by monkey C to target 2. Entry of the control cursor into the peripheral target marked the end of the trial. (c) Normalized coupling torque impulse at the shoulder vs. elbow per target during control and cerebellar block. For each session, we computed the target-wise median coupling torque impulse during the acceleration phase of the movement across the control and cerebellar block trials. They were then normalized by the maximum absolute torque impulse across all the targets. The depicted values are the means across all the sessions pooled from the data of all four monkeys. The 95% confidence interval of the means is indicated by the horizontal and vertical bars for the shoulder and elbow joints respectively.(d) Change in peak hand velocity due to cerebellar block plotted against the coupling torque in control for each session for the reaching movements (T1-4). The target-wise reduction in the median peak hand velocity during the cerebellar block trials was computed relative to that of control trials. The target-wise median coupling torque during the control trials of each session was normalized to the median across all trials of all sessions per monkey. The depicted data contains all the sessions pooled from all four monkeys. The black line overlayed on the scatter indicates the least-squares linear regression fit to the data points. [T1-8: Targets 1-8]

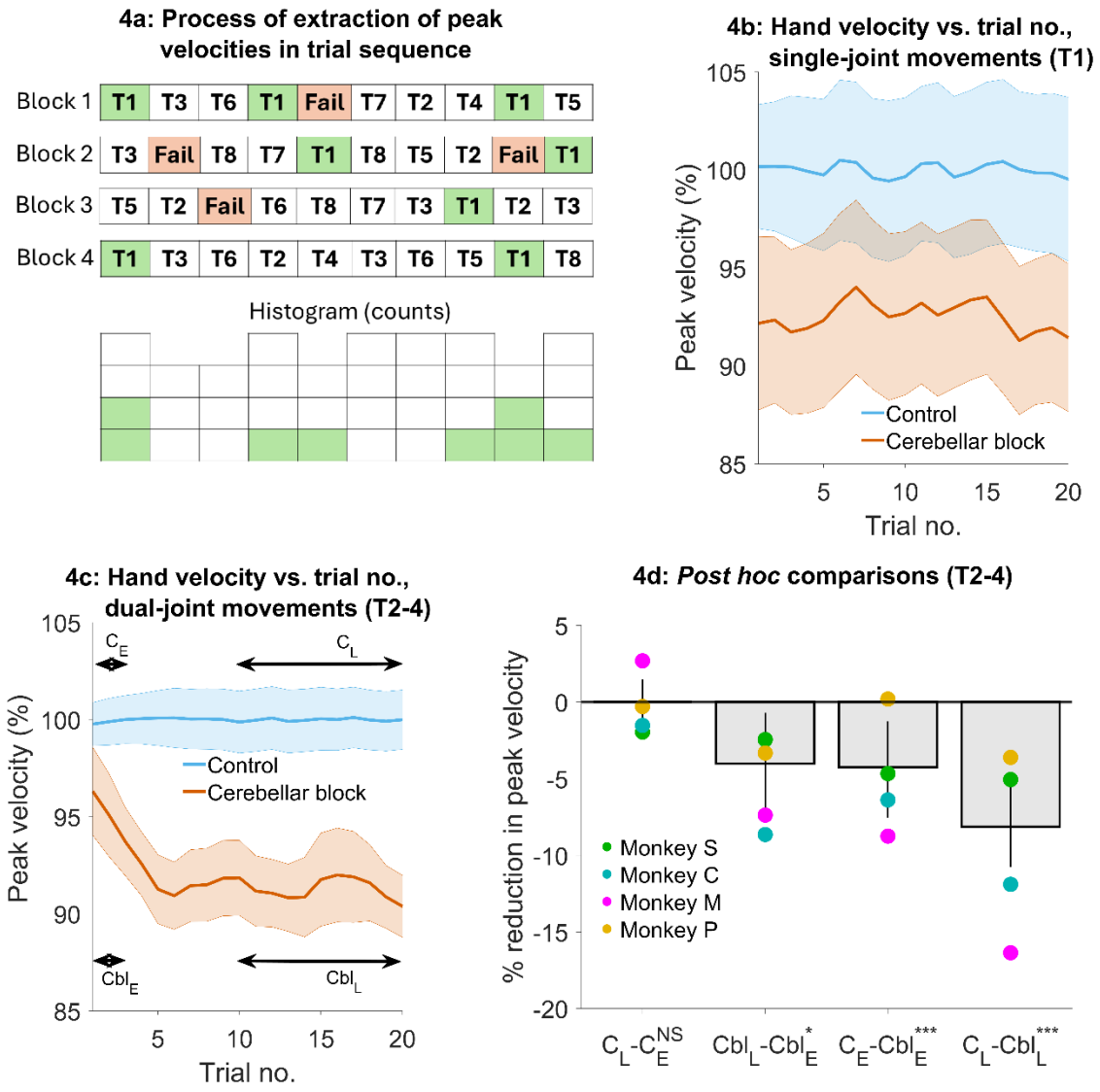

Figure 4: Effect of the cerebellar block on hand velocity across successive trials. (a) Schematic of the process of extraction of peak hand velocity for movements to a particular target from blocks of control/cerebellar block trials while preserving the order in which the target was presented. For each block, the peak velocity for movements to a particular target (in this example target 1) was extracted while retaining the trial numbers in which it was presented in the block. This enabled us to examine the evolution of the peak velocity across the sequence of presentation of the target during control vs. cerebellar block. (b) Mean ± 95% confidence intervals of the peak hand velocity for movements to target 1 across all the trial blocks pooled from all four monkeys. For each monkey, the peak hand velocities were normalized to the median peak velocity of the early trials 1-2 from all the control blocks. (c) Same as in (b) but for targets 2-4. (d) *Post hoc* comparisons between early trials 1-2 and late trials 11-20 during control and cerebellar block. Statistical significance is denoted as follows: $p \geq 0.05^{NS}$, $p < 0.05^{*}$, $p < 0.01^{**}$, $p < 0.001^{***}$. [E: Early, L: Late, C: Control, Cbl: Cerebellar block; T1-8: Targets 1-8]

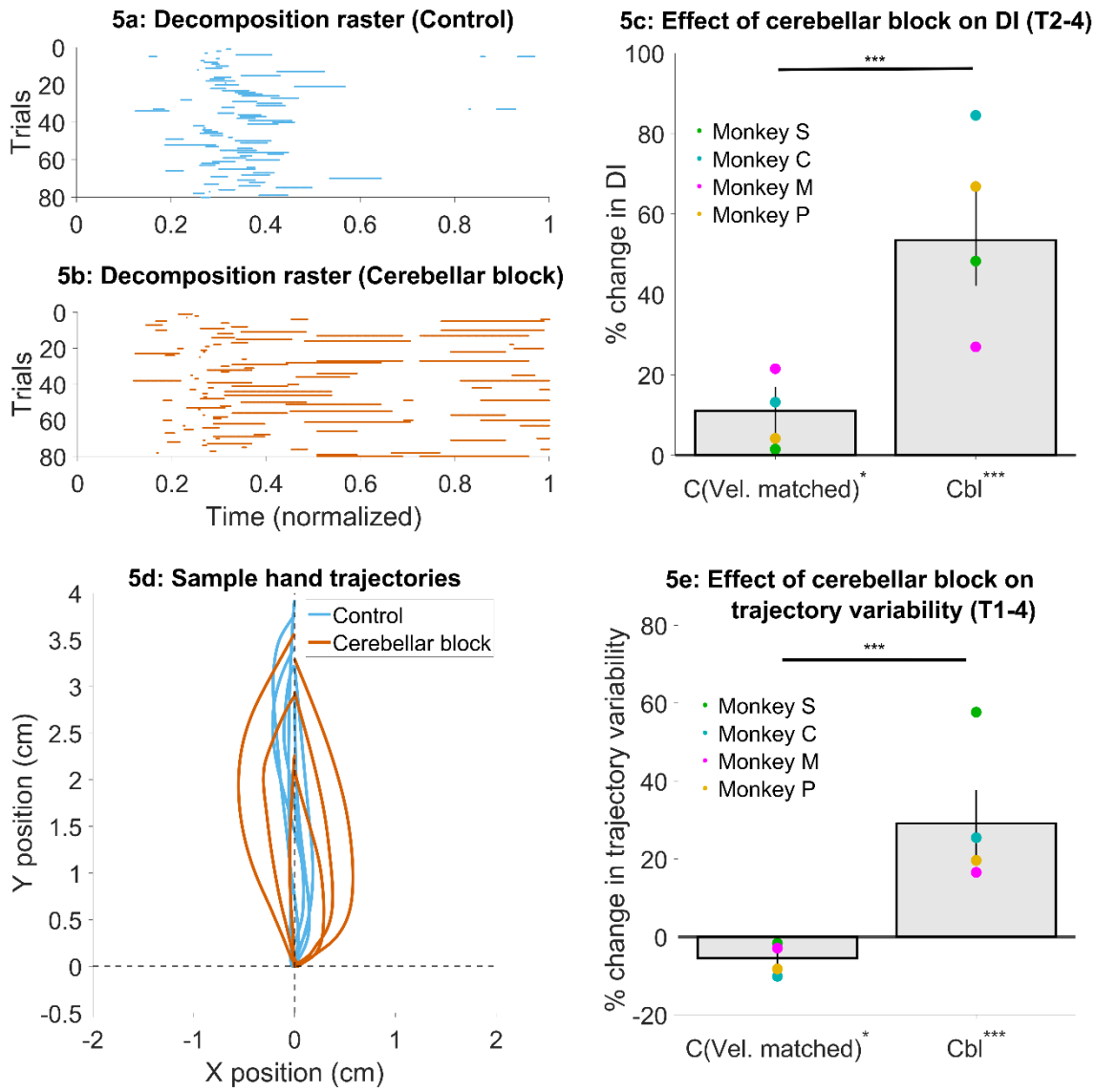

Figure 5a-c: Effect of the cerebellar block on the decomposition of dual-joint movements. (a) Binary decomposition raster of sample trials for movements made to target 2 by monkey C during control. The duration of each trial was normalized to 0-1 (bin width = 0.001) and then decomposition was computed for each bin based on whether either (but not both) of the shoulder or the elbow joint velocity was less than 20°/s. (b) Same as in (a) but for movements to target 2 by monkey C during cerebellar block. (c) Change in decomposition index (i.e., the proportion of the movement time during which the movement was decomposed, as defined above) for movements to targets 2-4 during velocity-matched control and cerebellar block trials relative to all control trials. The change in median decomposition was computed for each session. The depicted values are the mean ± 95% confidence intervals across all sessions pooled from all four monkeys. The individual means of each monkey are overlaid. **Figure 5d-e: Effect of the cerebellar block on inter-trial trajectory variability.** (d) Sample hand trajectories during control vs. cerebellar block trials for movements to target 2 by monkey C. The starting point of the trajectories was shifted to the origin and then they were rotated about the origin so that their endpoints lie on the positive Y-axis. (e) Change in Inter-trial trajectory variability for movements to targets 2-4 during velocity-matched control and cerebellar block trials relative to all control trials.

The trajectory variability was measured as the standard deviation of the maximum perpendicular distance of the trajectories from the Y-axis after transforming them as in (d). The change in trajectory variability for the cerebellar block trials was computed relative to the control trials for each session. The depicted values are the mean ± 95% confidence intervals across all sessions pooled from all four monkeys. The individual means of each monkey are overlaid. Statistical significance is denoted as follows: $p \geq 0.05^{NS}$, $p < 0.05^{*}$, $p < 0.01^{**}$, $p < 0.001^{***}$. [C: Control, Cbl: Cerebellar block; T1-8: Targets 1-8; DI: Decomposition index]